ChemSusChem

Research Article
doi.org/10.1002/cssc.202202361

Chemistry Europe
European Chemical Societies Publishing

www.chemsuschem.org

Recycling of All-Solid-State Li-ion Batteries: A Case Study of the Separation of Individual Components Within a System Composed of LTO, LLZTO and NMC

Aamir Iqbal Waidha,*[a] Amila Salihovic,[b] Martine Jacob,[b] Vanita Vanita,[b] Burak Aktekin,[c] Kristina Brix,[d] Kerstin Wissel,[a] Ralf Kautenburger,[d] Jürgen Janek,[c] Wolfgang Ensinger,[a] and Oliver Clemens*[a, b]

With the current global projection of over 130 million electric vehicles (EVs), there soon will be a need for battery waste management. Especially for all-solid-state lithium-ion batteries (lithium ASSBs), aspects of waste management and circular economy have not been addressed so far. Within such ASSBs, the use of solid-electrolytes like garnet-type $Li_{6.5}La_3Zr_{1.5}Ta_{0.5}O_{12}$ (LLZTO) may shift focus on strategies to recover not only the transition metal elements but also elements like La/Zr/Ta. In this work, we present a two-step recycling approach using citric acid as the leaching agent to separate and recover the individual components of a model cell comprising of $Li_4Ti_5O_{12}$ (LTO) anode, $Li_{6.5}La_3Zr_{1.5}Ta_{0.5}O_{12}$ (LLZTO) garnet electrolyte and $LiNi_{1/3}Mn_{1/3}Co_{1/3}O_2$ (NMC) cathode. We observe that by adjusting the concentration of citric acid, it was possible to separate the materials from each other without strong mixing of individual phases and also to maintain their principle performance characteristics. Thus, the process developed has a potential for upscaling and can guide towards considering separation capability of battery components in the development of lithium ASSBs.

Introduction

Energy storage devices based on Li-ion batteries have found application not only in small portable electronic devices like smart watches and phones, but also large scale application like electric vehicles (EVs).[1] The conventional Li-ion batteries use organic liquid electrolytes, which are not only flammable but also susceptible to Li dendrite growth that are both a major safety concern.[2] Lithium ASSBs based on solid electrolyte (SE) offer a viable alternative due to their high mechanical strength, high ionic conductivity, and the possibility to use lithium metal at the anode side, making them highly investigated alternatives,[3] and a strong candidate to enter the market in the near future. Lithium ASSBs can be constructed in general in two different types depending on the anode material used: The lithium metal SSB would have an increased energy density as compared to conventional batteries, whereas the lithium-ion SSB might benefit from shorter charging times and higher performance due to a transport number of 1 for the lithium ion reducing polarization.[4]

Within the ASSBs, both organic and inorganic electrolytes are of interest. As organic electrolytes, polymer electrolytes based on polyethylene oxide (PEO),[5] polyacrylonitrile (PAN),[6] polycaprolactone (PCL),[7] poly(methyl methacrylate),[8] have gathered wide spread interest due to favorable mechanical properties and partial self-healing capabilities.[9] On the other hand, inorganic electrolytes[10] based on sulfides[11] and oxides are of interest due to their high ionic conductivity and high lithium ion transference number.[3a] For the latter, oxide-based garnet electrolytes such as $Li_{6.5}La_3Zr_{1.5}Ta_{0.5}O_{12}$ (LLZTO)[12] are promising due to their stability towards the lithium metal anode,[3a,13] at the cost of ease of assembly and cycling stability due to mechanical properties. In addition, composite electrolytes made of a polymer electrolyte with inorganic fillers (both lithium-ion conductive and insulating)[6,14] have also received interest, but can suffer from issues of interfacial stability between the components leading to high lithium ion transference resistance at the polymer/filler interface.[5,15,16] along with low lithium ion transference numbers.[17] Therefore, the use of the different materials for ASSBs is critically discussed at

[a] Dr. A. I. Waidha, Dr. K. Wissel, Prof. Dr. W. Ensinger, Prof. Dr. O. Clemens
Fachbereich Materialwissenschaft, Fachgebiet Materialanalytik,
Technische Universität Darmstadt
Alarich-Weiss-Straße 2, 64287 Darmstadt (Germany)
E-mail: aamir.waidha@gmail.com
[b] A. Salihovic, M. Jacob, V. Vanita, Prof. Dr. O. Clemens
Institut für Materialwissenschaft, Chemische Materialsynthese,
Universität Stuttgart
Heisenbergstraße 3, 70569 Stuttgart (Germany)
E-mail: oliver.clemens@uni-stuttgart.de
[c] Dr. B. Aktekin, Prof. Dr. J. Janek
Institute of Physical Chemistry & Center for Materials Research,
Justus-Liebig-Universität Giessen
Heinrich-Buff-Ring 17, 35392 Giessen (Germany)
[d] Dr. K. Brix, Dr. R. Kautenburger
Anorganische Festkörperchemie,
Universität des Saarlandes
Campus, Gebäude C4 1, 66123 Saarbrücken (Germany)

Supporting information for this article is available on the WWW under https://doi.org/10.1002/cssc.202202361

This publication is part of a joint Special Collection on Solid State Batteries, featuring contributions published in Advanced Energy Materials, Energy Technology, Batteries & Supercaps, ChemSusChem, and Advanced Energy and Sustainability Research.

current and different materials might make it (or not make it) to the market within the next decade.[18]

With batteries becoming dominant in electric vehicles in the very near future (by 2040, 58% of the vehicles sold are estimated to be EVs)[19]), it will be important to have recycling strategies available and to consider resource availability, supply and finally the disposal. For conventional LIBs with liquid electrolytes, recycling strategies have been developed (though they need to be improved), which are based on a disassembly of the battery followed by hydrothermal treatment in inorganic or organic acid.[20] Special focus lies on the recovery of the elements from the cathode material, e.g., the transition metals from lithium nickel manganese cobalt oxide (NMC).[21] However, the design of recovery strategies is not only important for conventional lithium batteries, and it is time to think what might come in the future to have recovery strategies available in case lithium ASSBs will enter the market.

The use of SEs such as LLZTO will immediately change criticality considerations for lithium ASSBs. Li, Co, Ta and rare earth elements have been listed as critical not only because of their demand, but also due to their uneven distribution around the world. Lithium, for example, is produced mainly by two countries around the world, i.e. Chile and China, accounting of 44% and 39% of the global supplies.[22] Similarly, Co used in high energy density cathodes like NMC is predominantly supplied from the Democratic Republic of Congo, accounting for 59% of global production, rare earths are mined almost exclusively in China and Ta is mined to about 36% in the Democratic Republic of Congo. With tons of battery materials reaching the end of life, supply chains will have to move from mined materials to recovered materials, in order to limit the exploitation of nature.

To date, there are not many reports on the development of recovery strategies for chemically complex mixtures of electrode materials together with solid electrolytes, though some theoretical considerations have been made.[23] Recently, our group investigated the recovery of the SE $Li_{7-3x}Al_xLa_3Zr_2O_{12}$ from a complex mixture with $LiFePO_4$ and $Li_4Ti_5O_{12}$ via a hydrometallurgical approach using HCl,[24] which resulted in the recovery of the SE with a low recovery rate. This resulted from the fact that the whole material mixture was fully dissolved at the beginning and co-precipitation led to an unfavorable redistribution of elements (e.g., formation of $LaFeO_3$).

To overcome the issue of elemental redistribution, an alternative strategy is required, which could allow for the stepwise separation of the different battery components with high purity at a high rate. Such approaches can in principle exploit concepts of dissolution thermodynamics as well as kinetics, thus are likely to depend on the specific material combination.

In this work, we report a modified hydrometallurgy process for the separation of three materials commonly used for ASSBLIBs, $Li_{6.5}La_3Zr_{1.5}Ta_{0.5}O_{12}$ (LLZTO) as the SE, $Li_4Ti_5O_{12}$ (LTO) as the anode material as well as $LiNi_{1/3}Mn_{1/3}Co_{1/3}O_2$ (NMC) as the cathode material. We show that a mixture of these three components can be well separated by optimizing leaching time, temperature as well as the concentration of citric acid by characterizing the recovered materials via X-ray diffraction, scanning electron microscopy and elemental analysis. Remarkably, the recovered materials still maintain their principle electrochemical functionality as found by an electrochemical impedance spectroscopy study of the SE as well as cycling the electrode materials against Li metal. In addition, we highlight the importance of improving these strategies further by determining the origin of a slight reduction in the SE conductivity via X-ray photoelectron spectroscopy.

Experimental Section

Material synthesis

Synthesis of $Li_4Ti_5O_{12}$

The $Li_4Ti_5O_{12}$ anode material was synthesized by solid-state synthesis according to a previous report.[25] Li_2CO_3 (Alfa Aesar, 99%) and TiO_2 (Alfa Aesar, 99.9%) were ball milled for 8 h at 500 rpm with zirconia balls and vials using isopropanol as dispersing agent. An excess of Li_2CO_3 (20%) was added to compensate lithium losses, which may occur during the calcination process. Afterwards, the mixture was calcined in an alumina crucible at 800 °C (with 3 °C min^{-1} heating/cooling rates) for 8 h in air.

Synthesis of $LiNi_{1/3}Mn_{1/3}Co_{1/3}O_2$

$LiNi_{1/3}Mn_{1/3}Co_{1/3}O_2$ was synthesized by solid state reaction according to a previously reported synthesis procedure.[26] Stochiometric amounts of Li_2CO_3 (Alfa Aesar, 99%), MnO (Sigma Aldrich, 99%), NiO (Alfa Aesar, 99%) and Co_3O_4 (Merck, 99%) were ball milled in isopropanol for 12 h at 500 rpm with an intermediate breaking of 10 min after 10 min milling interval in order to avoid local increase of the temperature during milling process using zirconia balls and vials. An excess of Li_2CO_3 (20%) was added to compensate lithium losses, which occurs during the calcination process. Subsequently, the mixture was calcined in an alumina crucible at 900 °C (3 °C min^{-1}) for 12 h in air.

Synthesis of $Li_{6.5}La_3Zr_{1.5}Ta_{0.5}O_{12}$

LLZTO with a composition of $Li_{6.5}La_3Zr_{1.5}Ta_{0.5}O_{12}$ was synthesized according to a previously reported procedure.[5] Li_2CO_3 (Alfa Aesar, 99%), La_2O_3 (Alfa Aesar, 99.9%), Ta_2O_5 (Alfa Aesar, 99%) and ZrO_2 (Alfa Aesar, 99%) were mixed in stoichiometric amounts and hand milled in a mortar for 15 min. An excess of Li_2CO_3 (20%) was added to compensate lithium losses, which may occur during the calcination process. Afterwards, the mixture was calcinated in an alumina crucible at 900 °C (3 °C min^{-1}) for 12 h in air, followed by an intermediate hand milling in a mortar for 15 min. Subsequently, the mixture was sintered at 1100 °C (3 °C min^{-1}) for 10 h in air.

Leaching in citric acid

To determine separation strategies for the individual battery materials, a model composite mixture was prepared by hand milling equal amounts of each material, LTO, NMC and LLZTO, for 15 min in the weight ratio of 1:1:1 with the overall weight of composite being 3 g. Citric acid solutions of different molarities were prepared by adding citric acid (monohydrate, Sigma Aldrich) of appropriate amount to deionized water. All the leaching experiments were performed at 95 °C with constant stirring using a magnetic stirrer to maintain a homogenous temperature through-

out the solution. A solid to liquid ratio of 0.03 g L^{-1} and 0.1 g L^{-1} was used during the leaching in 0.2 M and 1.5 M citric acid solution. After the leaching process, filtration was carried out using the VWR qualitative filter paper 303 (particle retention 2–3 μm), followed by washing the residue three times with deionized water and subsequent drying at 100 °C. The filtrate was subjected to solvent evaporation, followed by a heat treatment of the obtained gel at 400 °C for 2 h in air. The obtained powders were then hand milled and subjected to a treatment at higher temperatures, where the detailed temperature depends on the material to be recovered (see section Development of a selective leaching process using citric acid).

To investigate the reproducibility of the recycling process, the experiments were performed three times followed by X-ray diffraction analysis (see next sub-section), which showed that the method is reproducible within the errors of the analysis method. The quantification error of the Rietveld method (see next sub-section) is usually within 1–2 wt% of the main phase. In addition, we also confirmed the capability for upscaling of the method on a batch of >10 g of materials mixture, which gave results in similar quality.

X-ray diffraction

X-ray diffraction (XRD) patterns were recorded with a Rigaku Smartlab device with a HyPix-3000 detector in Bragg–Brentano geometry with a Cu-K_α source operated at 40 kV and 30 mA. The total scan time was set to 1 h for the angular range between $10° \leq 2\theta \leq 80°$ at a step size of 0.005° and a fixed divergent slit with 0.3°. Phase quantification and characterization was performed using the Rietveld method within a fundamental parameters approach as implemented in TOPAS V6 (Bruker AXS, Germany).

Electrochemical impedance spectroscopy

Alternating current (AC) electrochemical impedance spectroscopy was carried out to characterize the conductivity of the as-synthesized and recycled LLZTO ceramics. For this, pellets were prepared by uniaxial pressing of as-prepared powders followed by sintering at 1100 °C for 12 h. The pellets were sputtered with a thin layer of gold on both sides for electronic contacting. The impedance measurements were carried out in the temperature range of 30 °C to 100 °C using an ITS unit (Biologic) connected to a MTZ-35 impedance analyzer (Biologic) by applying an AC signal of 100 mV amplitude with the frequency ranging from 1 MHz to 100 mHz. Fitting of the data was performed using RelaxIS (rhd instruments, Germany).

Galvanostatic cycling

Both NMC and LTO were tested in the half cell mode against a Li metal anode. The electrodes were prepared by mixing the active material with carbon black and polyvinylidene difluoride (PVDF) weight ratio corresponding to 80:10:10. The obtained slurry was deposited on Al foil and dried in the vacuum oven at 100 °C for 12 h. 7.9 mm diameter cathode chips were cut from the coated foil with the active material loading of 0.01256 mg for LTO and 0.00352 mg for NMC. All the electrochemical cell were loaded, sealed in the Swagelok cell inside the Ar glovebox. The Swagelok cells were assembled with the cathodes, metallic lithium as counter electrode and the liquid electrolyte. However, the sealed cells were operated outside the glovebox. The assembled cells were heated at 50 °C and were cycled in a constant current by using VSP 300 potentiostat from Biologic. All voltages are given as potential against the Li anode material. Voltage window cycling was performed under identical charging conditions with the cutoff voltages at 4.2 V for NMC; 2.7 V for LTO on charge window opening and at 3 V for NMC; 1 V for LTO on discharge window opening. The electrochemical experiments were performed with the charging and discharging currents of 52.8 μA for NMC and 219.9 μA for LTO. Note that charge/discharge current density corresponds roughly to C/10.

X-ray photoelectron spectroscopy

Sample were prepared in an argon glove (MBraun, $p(O_2)/p$ and $p(H_2O)/p < 0.1$–1 ppm) and the samples were transferred into PHI5000 Versa Probe II system (Physical Electronics GmbH) using an airtight transfer module. During measurements, Al-K_α radiation (1487.6 eV) was used and charge compensation was applied through a dual beam charge compensation system. During measurements, the pass energy was 23.5 eV, step size was 0.2 eV and step time was 50 ms. Unless specified, depth profiling and surface cleaning was not performed. Casa XPS was used for the data evaluation and a linear energy calibration was performed so that the hydrocarbon peak was positioned at 284.8 eV. Shirley background subtraction and intensity normalization (divided by the maximum) was applied in the reported spectra for an easier comparison of samples.

Inductively coupled plasma mass spectrometry

Mass spectrometry with inductively coupled plasma (ICP-MS) was conducted with a commercial ICP-MS system (8900 triple quadrupole ICP-QQQ and SPS4 autosampler, Agilent, USA). Single element ICP-MS standards of 1 g L^{-1} Li^+, Al^{3+}, Sc^{3+}, Ho^{3+}, Zr^{4+} (all Merck Millipore, Germany, $c(Zr^{4+}) = 10$ g L^{-1}), Mn^{2+}, Co^{2+}, Ni^{2+} (all Sigma–Aldrich, USA), La^{3+}, Ta^{5+} (all Alfa Aesar, USA) and Ti^{4+} (VWR, USA) were used. The measured isotopes were ^{7}Li, ^{27}Al, ^{47}Ti, ^{55}Mn, ^{59}Co, ^{60}Ni, ^{90}Zr, ^{139}La,^{181}Ta and as internal standards ^{45}Sc and ^{165}Ho. Except for ^{7}Li and ^{90}Zr, all isotopes were measured using He as collision gas to avoid possible disturbances. The detector dwell time was 100 μs and repetition was three times.

Scanning electron microscopy

Samples were sputtered with a 2–3 nm layer of Iridium (SCD 500, BAL-TEC). SEM images were taken with a dual beam FEI SCIOS FIBSEM at 30 kV and 6.4 nA.

Results and Discussion

Development of a selective leaching process using citric acid

The selective leaching of individual components from a mixture of LTO, LFP and $Li_{7-3x}Al_xLa_3Zr_2O_{12}$ using the mineral acid HCl was reported to be unsuccessful as a consequence of unfavorable co-precipitation of elements, which were contained in two separate battery components prior, e.g., La and Fe within $LaFeO_3$.[24] A similar behavior was observed for the composite mixture of LTO, NMC and LLZTO with mineral acids and we noted the co-precipitation of La from LLZTO with transition metals (Ni, Mn, Co) from NMC on increasing the pH of the solution, resulting in the formation of very stable perovskite-type materials. Thus, additional steps would be required to

separate these materials and recover the individual components. Organic acids such as citric acid have a lower acidity, which can result in different dissolution kinetics. In addition, they have different complexation behavior with transition metals vs. trivalent lanthanides,[27] which could also help to selectively leach certain compounds from each other. Further, they are easier to handle, being less corrosive and they have lower environmental fingerprint.

The starting materials LLZTO, LTO and LCO were characterized by powder diffraction and were found to be basically phase pure, with LLZTO containing a small amount of impurity phase (Figure 1),. The lattice parameters agree with data in literature,[28] confirming successful synthesis (NMC (*R*-3*m*): $a=$ 2.8543(1) Å, $c=14.2076(5)$ Å; LTO (*Fd*-3*m*): $a=8.3606(1)$ Å; LLZTO (*Ia*-3*d*): $a=12.9370(1)$ Å). For NMC, the composition could be further verified by chemical analysis using emission spectroscopy (later in this article).

The materials were then mixed by hand milling in order to form a model black mass, which could be considered as an intermediate product in a recycling process after removal of the housing and current collectors. At this point, certain aspects should be acknowledged: In a full battery cell (depending on the detailed strategy used for assembling), the electrode materials would likely be further mixed with additives such as binders like PVDF[21a] and carbon for enhancing the electronic conductivity.[26] Additionally, components may be in part sintered together to form even, smoother and well connected interfaces.[29] Further, in lithium ASSBs, solid electrolyte interfaces (SEI) may also form on cycling, which could result in partial mixing or compositional changes at these interfaces.[3a] All these processes would complicate the separation of a mixture further and it is thus important to emphasize that our study here presents a feasibility approach for the selective leaching on a simplified model system.

From our previous experience, NMC is the material which can be dissolved much easier as compared to LTO and LLZTO. Thus, before approaching the material mixture, the solution behavior of NMC and the other materials towards aqueous solution of citric acid was investigated, emphasizing aspects of the solution molarity and leaching duration, in order to find the most efficient conditions. Different citric acid solutions (4, 2, 0.2 and 0.1 mol L^{-1}) were used for leaching NMC for 8 h at 95 °C. It was observed that NMC could be completely dissolved in solution with concentrations of citric acid larger than 0.1 mol L^{-1}, whereas about 23% of NMC remained undissolved for the 0.1 mol L^{-1} concentrated solution. Further, we found that the leaching duration can also be reduced to 4 h for the complete dissolution of NMC at this concentration, whereas lowering the leaching temperature resulted in longer leaching durations in order to obtain complete dissolution of the NMC powders. The experiments were repeated at least three times to verify these results and could be reproduced within errors. From the determined reproducibility, the temperature of 95 °C was kept constant for further leaching attempts.

Subsequently, we studied the dissolution behavior of LLZTO, which was easier to dissolve than LTO from our previous experience. For leaching in 0.2 M citric acid for 4 h at 95 °C, we found that LLZTO is fairly stable, with the filtration residue amounting to approximately ~85 wt% of the initial material. From the Rietveld analysis of the X-ray diffractogram of the resulting residue we observed that the powder represents a phase mixture of LLZTO and the fluorite/pyrochlore type La_{2+}

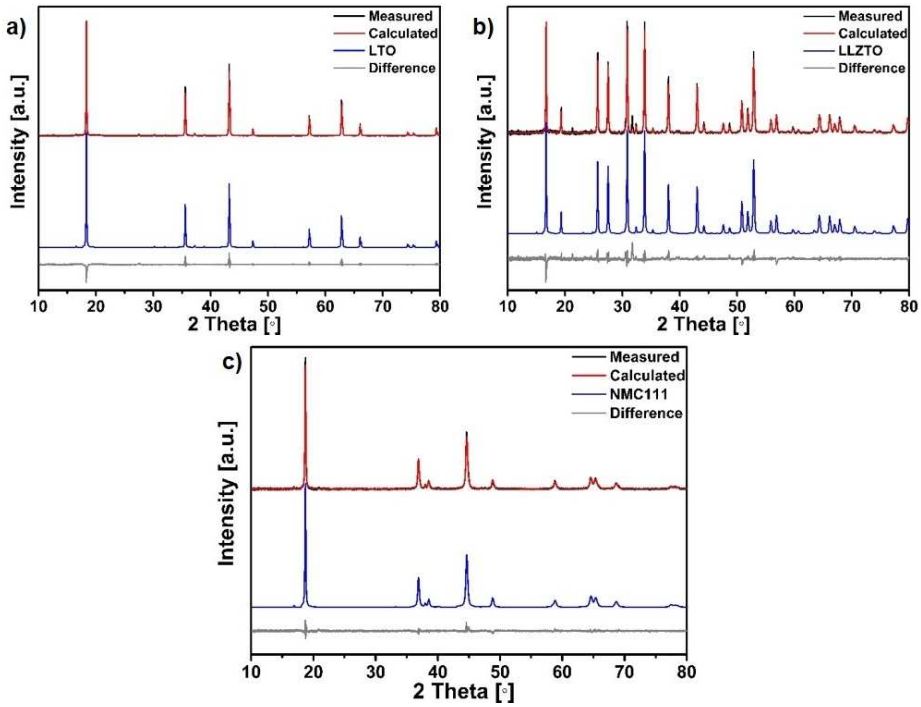

Figure 1. Rietveld fit of the powder X-ray diffraction data for as-synthesized a) LTO, b) LLZTO, and c) NMC.

$_xZr_{2-x}O_{7-x/2}$[30] (potentially Ta-doped,[31] thus described as $La_{2+x}Zr_{2-x}O_{7-x/2}$/Ta in the following), which is a well-known impurity phase found within the garnets due to Li loss. This indicates that during leaching in 0.2 M citric acid, Li loss likely takes place within the LLZTO structure, most likely initiated via a H^+/Li^+ exchange, and this is well known for Li containing compounds as well as garnets.[32] This also indicates that Li_2O from LLZTO is transferred into the solution; presumably, the resulting $La_{2+x}Zr_{2-x}O_{7-x}$ forms a barrier which slows down the degradation process of the underlying LLZTO. The results hence indicate that, within the possible two component mixture of NMC and LLZTO, NMC would dissolve first and LLZTO would remain as the residue with a partial reduced Li content.

In addition, we attempted to dissolve LTO in 0.2 mol L^{-1} citric acid at 95 °C for 4 h, which did not result in considerable mass loss. Thus, this approach could be used to separate NMC from LLZTO and LTO without additional dissolution of metals other than Li from the latter two components and we emphasize that lithium precursors are used in excess during the synthesis of battery materials to compensate for losses on heating. Nevertheless, even if NMC can be removed from this composite mixture of LTO/LLZTO/NMC, the remaining residue would contain LTO and LLZTO. Hence, we further optimized the leaching conditions for the dissolution of LLZTO from this LTO/LLZTO two component system.

Consequently, the mixture of LTO/LLZTO was subjected to leaching in higher molar citric acid solutions (0.5, 1.0, 1.5 mol L^{-1}) for 24 h at 95 °C. Quantification of this mixture by Rietveld analysis is complicated from the fact that both materials have large crystallite sizes and LLZTO has a higher absorption coefficient than LTO, which leads to a strong over quantification of low-absorbing LTO (weight ratio of LLZTO/LTO ≈25:75 for optimal prepared XRD samples (i.e., finely ground) instead of 50:50 as expected from original weights (Figure S2 in the Supporting Information). To make sure that this misquantification does not result from the presence of amorphous phases within LLZTO, we performed a quantification of amorphous phases via an internal standard approach by adding to both starting materials LTO and LLZTO the similarly absorbing materials Al_2O_3 and LaB_6, respectively. From this, we could confirm full crystallinity of both LTO and LLZTO starting materials (see Figures S2 and S3 and Information given in Supporting Information). For the 0.2 mol L^{-1} concentration of citric acid, the observed weight ratio of LTO/LLZTO is similar to that of the 1:1 starting mixture, confirming that only a low degree of dissolution of LLZTO takes place. Once the molarity of the citric acid solution increases, the reflection intensity of LLZTO, which correlates with the weight fraction of the phase within the residue, decreases. For the leaching in 1.5 M citric acid solution, we found from the X-ray diffraction that the residue only contains the mixture of LTO along with TiO_2. The presence of TiO_2 within the residue suggests the dissolution of Li_2O from LTO. However, the results indicate that a separation of LLZTO from LTO becomes feasible on increasing the concentration of citric acid.

Following this optimization, the three-component model mixture of LTO/LLZTO/NMC was subjected to a two-step citric acid leaching aiming to a step-wise separation of components. First, 3 g of this mixture were subjected to acid leaching in 0.2 M citric acid solution for 4 h at 95 °C (Figure 2a). After

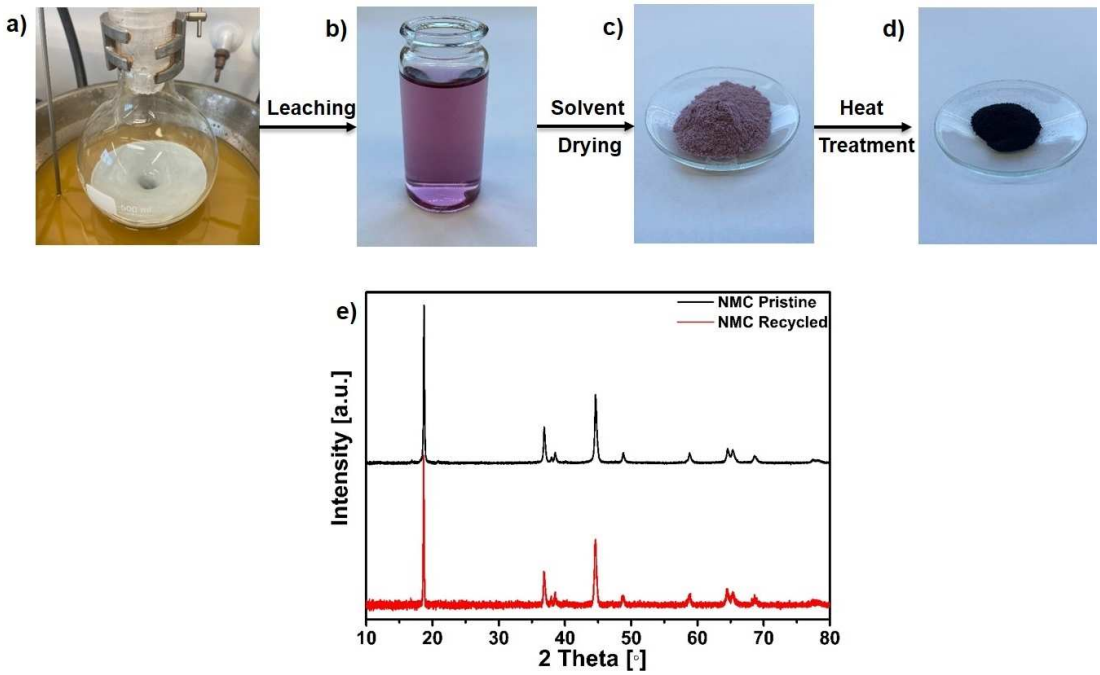

Figure 2. a–d) Photographs showing the intermediate products leaching of LTO/LLZTO/NMC mixture in 0.2 M citric acid solution followed by purple filtrate which after drying leads to purple powder and finally black mass power after high temperature heat treatment at 900 °C. d) Comparison of the X-ray diffractogram of the pristine NMC and recycled NMC.

leaching, the solution was filtrated leaving behind the residue (not shown) and the filtrate (Figure 2b). In a conventional hydrometallurgy processes, after acid leaching metal salt precipitation is carried out by adjusting the pH of solution.[21a] However, within the approach presented here, we simply carry out a solvent evaporation treatment at 100 °C, which leads to the formation of a gel. This gel was ground and heated at 400 °C for 2 h in order to remove organic residues. The obtained powder (Figure 2c) was then heated at 900 °C for 12 h, after which 0.99 g of a black powder (Figure 2d) were obtained. From the XRD pattern recorded on this black powder (Figure 2e), we observed that the diffraction profile is similar to that of pristine NMC and, from the Rietveld analysis, the calculated lattice parameters were found to be similar to that of pristine NMC (Table 1).

Further, ICP-MS measurements were carried out on both the pristine as well as the recycled NMC. Importantly, the molar ratios between Li/Ni/Mn/Co are maintained and we could not identify significant amounts of these metals contained in LTO or LLZTO (see ICP results in Table 2) to be transferred to the recovered NMC. However, we acknowledge the occurrence of Al, likely introduced from the use of alumina crucibles. Regardless of this, doping of NMC with Al does not defunctionalize the material and can even be used to stabilize the electrochemical performance of NMC cathodes.[33]

We also compared the XPS spectra for pristine and recycled NMC. The XPS spectra of the both pristine and recycled NMC are very similar for all the transition metals as well as the lithium (see Figure 3). Due to the spin-orbit coupling, the Co 2p signal splits into Co $2p_{3/2}$ and Co $2p_{1/2}$ (Figure 3a) with an intensity ratio of to 2:1. The Co $2p_{3/2}$ component was found to be at 779.7 eV along with a satellite peak of ~10% relative intensity located at nearly 10 eV higher binding energy. This supports the presence of Co in its trivalent oxidation state.[34] In the case of Mn (Figure 3b), Mn $2p_{1/2}$ and Mn $2p_{3/2}$ peaks are observed at 653.6 eV and 641.8 eV, respectively, while a contribution of Ni Auger peak (Ni LMM) is also observed resulting with a lower energy shoulder. In Ni 2p spectra (c), the Ni $2p_{3/2}$ peak is observed at 854.6 eV and the corresponding satellite peak at 861 eV. Similar arguments provide further support of Mn being present in its tetravalent oxidation state[35] and Ni being present in its divalent oxidation state[36] as expected for the layered NMC111 material.[37]

We would like to emphasize that the citric acid dissolution process followed here resembles a citric acid sol-gel based synthesis, which has been previously reported for NMC

Table 1. Comparison of lattice parameters of the pristine and recycled materials obtained from Rietveld refinements.

Sample	Space group	Lattice parameter [Å]	
		a	*c*
Pristine NMC	*R*-3*m*	2.8543(1)	14.2076(5)
Recycled NMC	*R*-3*m*	2.8539(1)	14.2308(15)
Pristine LLZTO	*Ia*-3*d*	12.9370(1)	
Recycled LLZTO	*Ia*-3*d*	12.9570(2)	
Pristine LTO	*Fd*-3*m*	8.3606 (1)	
Recycled LTO	*Fd*-3*m*	8.3594(1)	

Table 2. Results of ICP-MS analysis for the chemical composition of recycled in comparison to as-synthesized (pristine) materials.[a]

Sample		Li	Mn	Co	Ni	Ti	Zr	La	Ta	Al
NMC	pristine	0.97	**1/3**	0.34	0.36	0.00	0.00	0.00	0.00	0.00
	recycled	1.12	**1/3**	0.34	0.36	0.00	0.00	0.01	0.00	0.01
LLZTO	pristine	9.43	0.00	0.01	0.00	0.04	1.39	**3**	0.21	0.29
	recycled	5.85	0.00	0.01	0.00	0.14	1.32	**3**	0.19	0.48
LTO[b]	pristine	**4**	0.00	0.00	0.00	1.41	0.00	0.00	0.00	0.00
	recycled	**4**	0.00	0.00	0.00	1.96	0.15	0.38	0.00	0.00

[a] The metal concentrations in solution were normalized to molar ratios relating to the sum formulas of the materials to make it comparable to the chemical formulas of the compounds for $Li_{6.5}\mathbf{La_3}Zr_{1.5}Ta_{0.5}O_{12}$ (LLZTO), $\mathbf{Li_4}Ti_5O_{12}$ (LTO) and $LiNi_{1/3}\mathbf{Mn_{1/3}}Co_{1/3}O_2$ (NMC). [b] For LTO, the large deviation of Ti content originates from the fact that the material could not be fully dissolved; to estimate a potential transfer of impurities, we assumed a full solubility of the lithium component and normalized to this species.

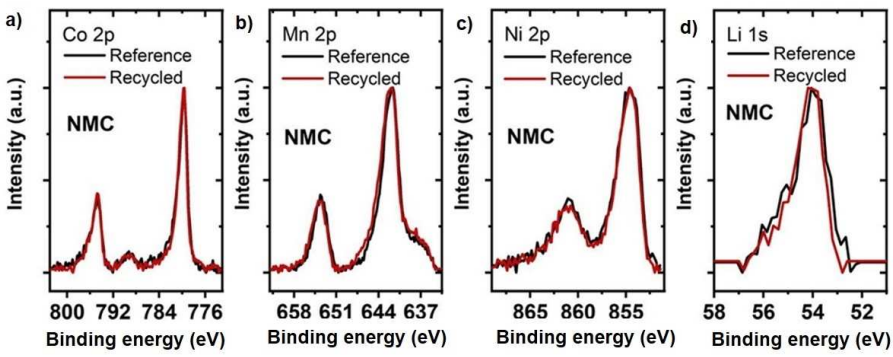

Figure 3. Comparison of the normalized XPS spectra of the transition metal ions within pristine and recycled NMC. Black line: Pristine NMC, Red: Recycled NMC.

preparation.[38] This is often beneficial to obtain small particle sizes, which can enhance the cycling behavior of the material and, indeed, this could be observed on comparing the cycling behavior of the pristine and recycled NMC (see section Electrochemical characterization). Remarkably, potential partial dissolution of Li_2O from LLZTO and LTO (as indicated from the increase of Li content from the ICP-MS analysis (see Table 2) helps to stabilize the desired NMC composition, so that no excess of a lithium precursor needs to be provided for the re-synthesis.

Following this, we processed the insoluble residue, which was left over after the removal of LTO/LLZTO. Rietveld analysis of powder diffraction data (Figure 4a) showed only the presence of LTO and LLZTO within the powders and no reflections belonging to NMC. Interestingly, no clear indication was given for the formation of $La_{2+x}Zr_{2-x}O_{7-x/2}$/Ta, which indicates that the dissolution of NMC and complexation of transition metal cations further prohibit the degradation of the other two components if the molarity of citric acid is sufficiently well adapted. The difference of phase fractions of LTO and LLZTO is well explained from the absorption contrast of LTO and LLZTO as discussed before and explained in more detail in the Supporting Information.

Subsequently, this mixture was subjected to a leaching step in 1.5 M citric acid solution for 24 h at 95 °C. After this leaching step, filtration was again carried out leaving behind a residue and yellow tinted filtrate (Figure 4b). The solvent was removed from the filtrate at 100 °C, followed by a heat treatment at 400 °C for 2 h to remove any organic impurities and a final high temperature heat treatment at 1000 °C for 12 h to obtain a white powder. The diffraction pattern was found to be similar to that of $La_{2+x}Zr_{2-x}O_{7-x/2}$/Ta (see Figure S1 in Supporting Information), which is a well-known impurity phase within the garnet materials due to Li loss.[16] This indicates that, though citric acid appears to be suitable to extract La/Zr/Ta, these materials are fairly stable. The required high reaction temperatures prohibit a simple re-synthesis of LLZTO due to a most likely increased volatility of Li, which is known to be transported from water residues likely originating from the ongoing destruction of C–H–O residuals and water formation on further heating. This has been observed in other solution based approaches for the synthesis of LLZTO as well.[39] Hence, additional Li-precursor was added to compensate this loss and the powders were heated again to 1000 °C for 12 h. From the Rietveld analysis of the obtained powder, it was confirmed that the resulting powder mainly consists of LLZTO and the lattice of the recycled compound, as determined by XRD, is basically identical to our pristine material (Table 2). In addition, ICP-MS measurements (Table 2) on both the pristine and recycled LLZTO were carried out in order to determine the presence of impurities, especially transition metal ions from the NMC. These impurities must be avoided, since they would lower the electrochemical operation window of LLZTO due to the redox

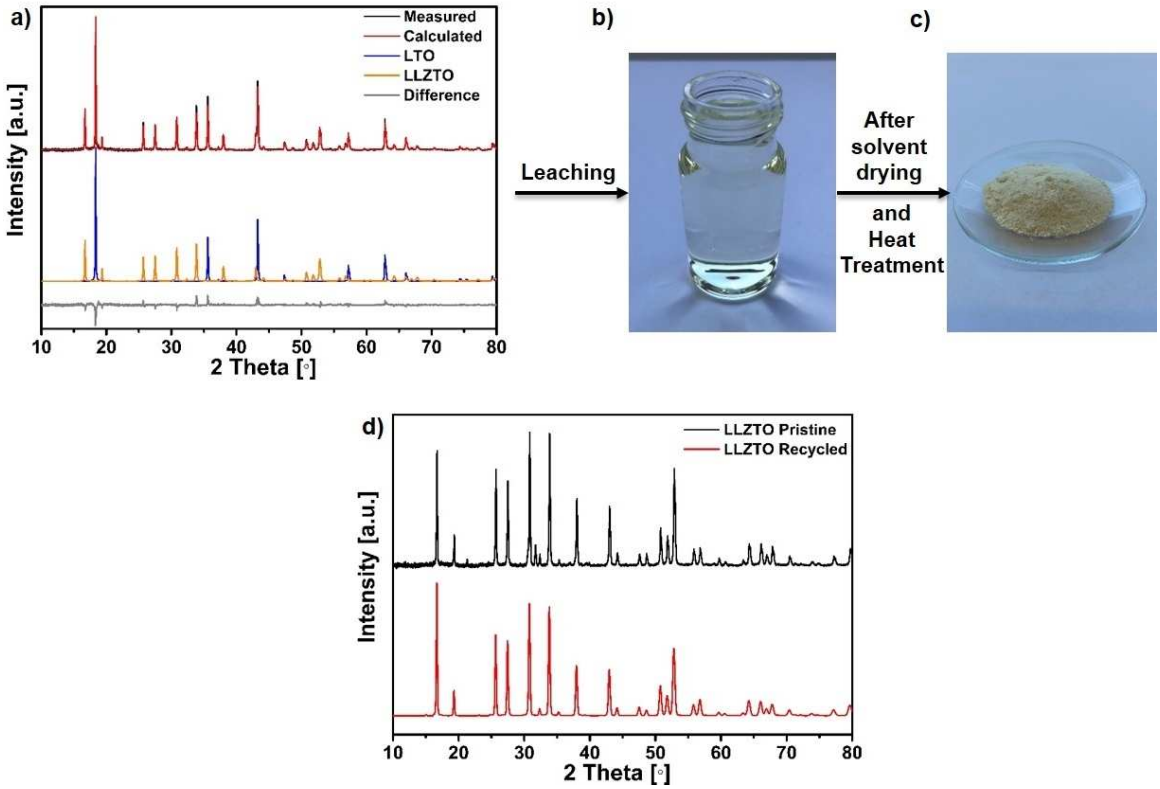

Figure 4. a) Rietveld fit of the X-ray powder diffraction data recorded on the powder residue after the 1st leaching step. b) Yellow tinted filtrate after 2nd leaching in 1.5 M citric acid. c) Powder obtained after solvent evaporation and subsequent high temperature heat treatment at 1000 °C. d) Comparison between the powder X-ray diffractograms of the pristine and recycled LLZTO.

activity of transition metals and might induce partial electronic conductivity into the SE. No indication was found for the presence of significant amounts of these transition metals, indicating that the washing of the residue after filtration of the first leaching step was sufficient. Since Li is used in excess for the synthesis process, deviations of, for example, the Li/La ratio are expected and found indeed for both pristine and recycled LLZTO. Nevertheless, the La/Ta/Zr ratio is maintained after the recycling process (the reduced Ta content in comparison to weighed Ta/Zr ratio likely originates from a lower solubility of Ta). Both the pristine and recycled LLZTO were found to contain Al, which is a known impurity induced from the use of alumina crucibles within the synthesis of LLZTO (see Table 2). The higher Al content in recycled LLZTO possibly originates due to additional heat treatment required for obtaining the recycled LLZTO from the second filtrate.

In a final step, we characterized the insoluble residue from the second leaching step (Figure 5). Analysis of diffraction data indicated that this phase only contained LTO without formation of TiO_2, indicating a complete removal of LLZTO from the mixture. The absence of obvious degradation of LTO is remarkable and needs further consideration. LLZTO is a basic oxide, significantly more basic than NMC due to its high lithium content. Thus, the complexation of La/Zr/Ta in addition to a reduction of the pH prevents the further degradation of LTO, which was observed on treating pure LTO at identical conditions. We emphasize that both pristine and recycled LTO could not be characterized completely using ICP-MS due to incomplete solubility of this material, which likely causes Ti being present in insoluble TiO_2 residues. It can be seen from Table 2 that some La and Zr from LLZTO seem to be transferred to the LTO or might not have dissolved completely, however, the overall content remains small, in agreement with the XRD pattern shown in Figure 5. This is also supported by the XPS analysis for LTO (see Figure 6), which indicates a strong dominance of Ti with signals at 464.1 eV and 458.3 eV corresponding to characteristic $Ti\,2p_{1/2}$ and $Ti\,2p_{3/2}$ peaks, respectively and indicating its presence in the tetravalent oxidation state.[40]

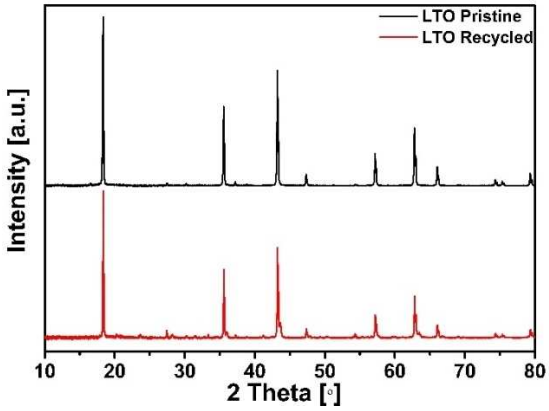

Figure 5. Comparison between the powder X-ray powder diffraction data recorded for pristine and recycled LTO.

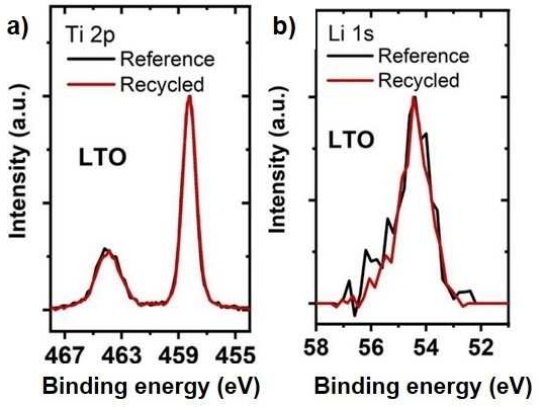

Figure 6. XPS spectra of the Ti 2p and the Li 1 s signals of LTO. Pristine (green) and recycled (red) materials are shown.

The flow chart of the overall recycling process developed here is presented in Figure 7. We emphasize that this process has significant advantages compared to the use of mineral acids. We observed excellent recovery of the respective materials and, from a pure elemental perspective, these approaches appear to be very promising regarding the separation of elements in such a way that they could serve for a simplified re-synthesis of the battery components. However, one must clearly distinguish from the determination of suitable separation approaches and the formation of best performing battery materials, which normally uses well characterized and pure products. Clearly, the processing of materials in complex mixtures can have adverse effects and requires a study of the principal electrochemical characteristics, which will be reported in the next section.

Further, we would like to emphasize that we have also scaled up the recycling approach to a batch of 10 g of materials. Within errors of phase quantification, the phases which could be identified after recycling are the same, showing that the process might be scaled without stronger modifications.

Electrochemical characterization

Electrochemical impedance spectroscopy of LLZTO

In order to determine the influence of the recycling process on the electrochemical performance of recycled LLZTO, impedance measurements were carried out on the recycled and pristine LLZTO. We do not want to benchmark a solid electrolyte, but it is important to examine intrinsic property changes which might be induced during the materials treatment. For both samples, the Nyquist plots (Figure 8a) show a depressed semi-circle at high and mid frequencies along with the capacitive response at low frequency, which indicates the blocking effect of the sputtered gold electrodes. This is further confirmed from the Bode plots, where two different phase dependences as a function of frequency can be seen (Figure 8b and c), indicating two transport processes. Hence, for both pellets, an equivalent circuit consisting of two R-CPE and a CPE element connected in

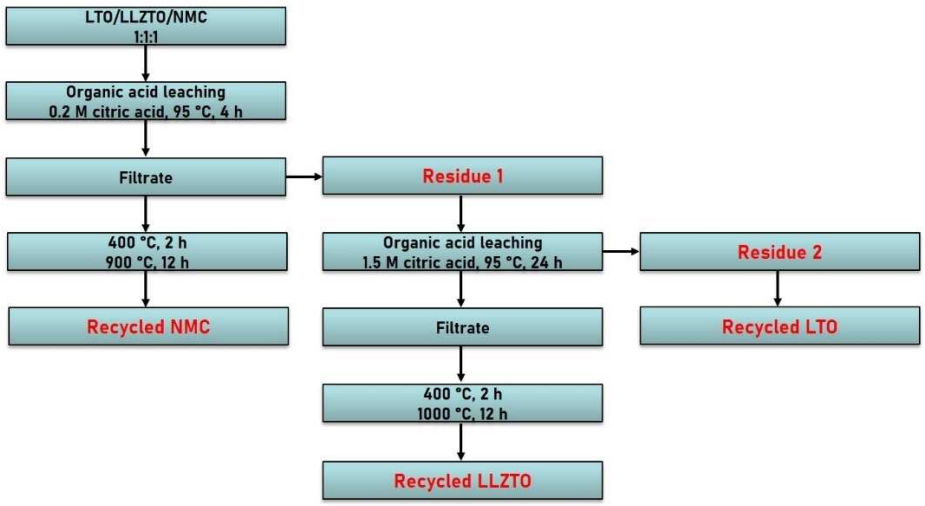

Figure 7. Flow chart of the recycling process.

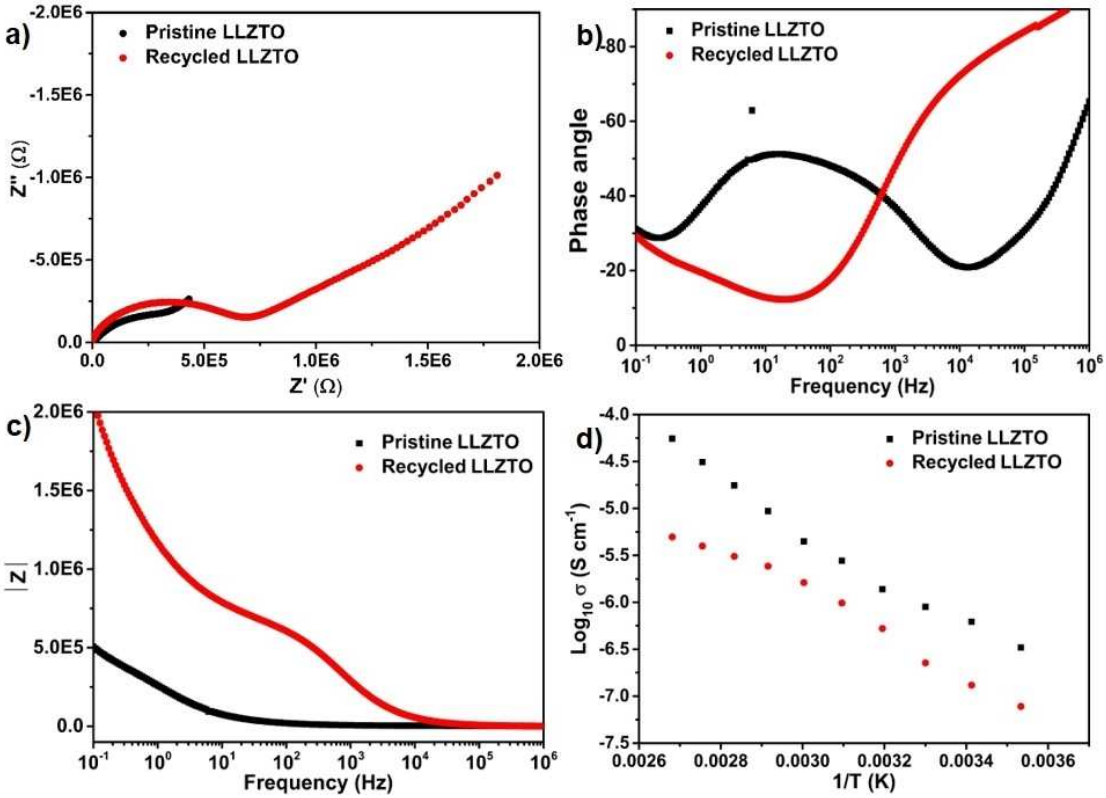

Figure 8. Comparison of the a) Nyquist plot, b,c) Bode plots and d) Arrhenius plot recorded for pristine and recycled LLZTO.

series was used to fit the impedance data and to determine an overall resistance and conductivity, respectively. The conductivities for pristine as well as recycled LLZTO are in the same order of magnitude at $8.95.10^{-7}$ S cm^{-1} and $2.26.10^{-7}$ S cm^{-1} at 30 °C, respectively. The lower conductivity of the pristine LLZTO could be related to lower sintering temperature and duration, which lowers the grain growth and density of the pellets and contributing to the lower ionic conductivity of the pristine pellet.[15,41] Nevertheless, since a similar procedure was used for the preparation of recycled pellet, a quantitative information on the role of the recycling process on the ionic conductivity can be obtained. The lower conductivity for the recycled material and its different behavior on heating could be explained from the fact that impurities transferred from the leaching process will likely accumulate at grain boundaries, and thus will affect the sintering of particles and/or provide additional grain

boundary resistances. Such an influence is in principle indicated in the SEM micrographs (see Figure 9), which indicated a finer microstructure of the recycled material, which will negatively impact a bulk ion conductor. Clearly, this aspect would have to be optimized in order to obtain a best functioning material. However, the fact that the conductivity can be mainly maintained at this stage can be considered promising for the further development and exploitation of the separation method presented here.

Characterization of the electrode materials NMC and LTO

The preparation of functional ASSB-LIBs is a current challenge and the use of garnet solid electrolytes has been found to be even more challenging with respect to achieving good cycling stability. Since, this study aims at the development of a recycling and separation process of battery components and not on making a highly functional ASSB-LIB. The pristine and recycled electrode materials were charged against lithium metal using established liquid electrolytes.

For the cycling of pristine NMC (Figure 10a), we observed that the material can in principle be charged and discharged within the potential window as reported in literature, though we did not achieve a comparable well-performing behavior.[42] This could be related to the grain size and lack of particle design of NMC powders used here that might inhibit accessing the full capacity in addition to handle these coarse materials well in electrode preparation. We would like to emphasize here, that the focus lies in the phase purity of the pristine materials used along with the possibility of obtaining them back in with as much purity as possible. Interestingly, we found that the recycled material performs different than our pristine material and could provide higher capacities, however at lower potential (Figure 10b). The detailed origin of this behavior requires further characterization. We assume that the changes of the shape and potential of the plateau are likely related to potential smaller impurities induced within the recycling process; in contrast, we think that the increase in capacity might be related to improved microstructural properties of the recycled NMC. The use of a simple solid-state approach for the synthesis of the pristine material resulted in large particle sizes for pristine NMC. In contrast, the recycling process resembles a citric-acid sol-gel route, which is known to be beneficial to achieve better performing electrode materials.[43] This is in part also indicated from a SEM analysis, which shows that though the primary particles are bigger for recycled NMC, the secondary particles, which comprise the larger particles, appear to be smaller (see Figure 11a and b). Further, the different behavior of recycled and pristine might result from smaller deviations of composition, which has been reported to impact the behavior of layered materials, e.g., for $Li_{1+x}(Ni_{1/3}Mn_{1/3}Co_{1/3})_{1-x}O_2$.[44]

For LTO, one might expect the smallest impact on the electrochemical behavior, since this material was basically undissolved in the process developed and only might modify its behavior due to impurities induced or due to partly dissolution of Li_2O at the grain boundary. Indeed, SEM micrographs indicate that the morphology of the sample is basically

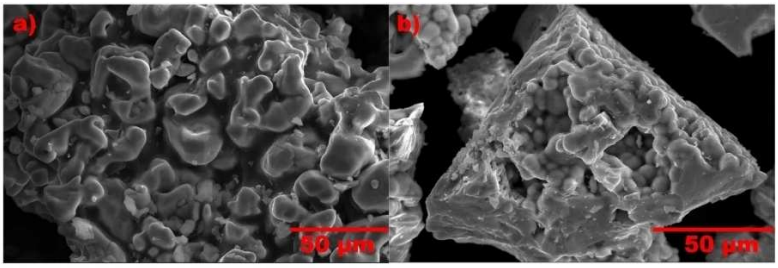

Figure 9. SEM micrographs of pristine (left) and recycled (right) LLZTO.

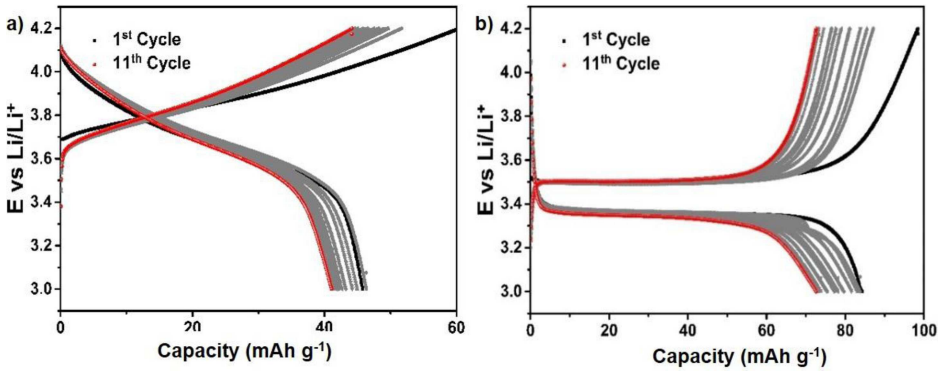

Figure 10. Comparison of electrochemical cycling of pristine (a) and recycled (b) NMC against metallic lithium.

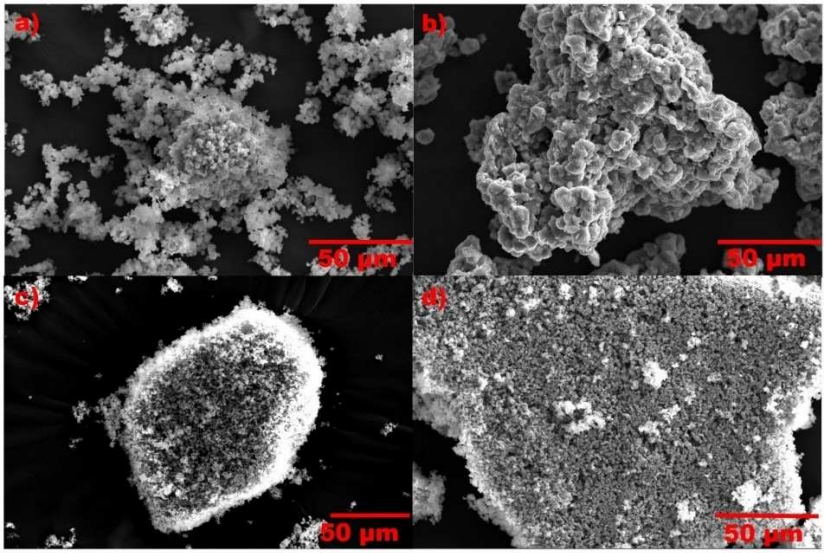

Figure 11. SEM micrographs of a) pristine NMC, b) recycled NMC, c) pristine LTO and d) recycled LTO.

maintained after the recycling process (see Figure 11b). We observed that the material maintains its electrochemical characteristics on charging and discharging against lithium metal (see Figure 12), though we did not achieve benchmarking characteristics as reported in literature. Again, this is likely related to the use of solid-state reactions for material synthesis, without applying a strong particle engineering. The differences observed between pristine and recycled materials are likely related due to the small amount of impurities induced to the recovered sample, which might alternate the detailed voltage characteristics and provide some additional surface resistances to the material leading to overpotentials, which affect the shape of the curves and lead to lower capacities.

Conclusions

Recycling of lithium ASSBs will become highly important once these batteries would enter the market and it is necessary to have a vision of principle recycling strategies to avoid accumulation of used, and potentially hard-to-be-recovered batteries at their end-of-life. The findings of these studies indicate that organic acids such as citric acid, which can act as complexing agent in addition to providing acidification, might be a key for the efficient separation of electrode materials from oxide anodes and electrode materials in lithium ASSBs. This leads to a strong improvement compared to our previous study in which we used HCl and obtained unfavorable mixing of cations from the different electrode components.[24] In comparison to conventional lithium ion batteries, this might even give the chance for maintaining the Li/M stoichiometry from the cathode material, since one could avoid Li residues from the use of liquid electrolytes, which might affect the re-synthesis potentially. However, one must clearly address that, though the findings presented here indicate the potential use of such a combination within a circular economy, it would still require significant improvement of the fabrication processes. Further, we emphasize that the use of coated particles, sintering

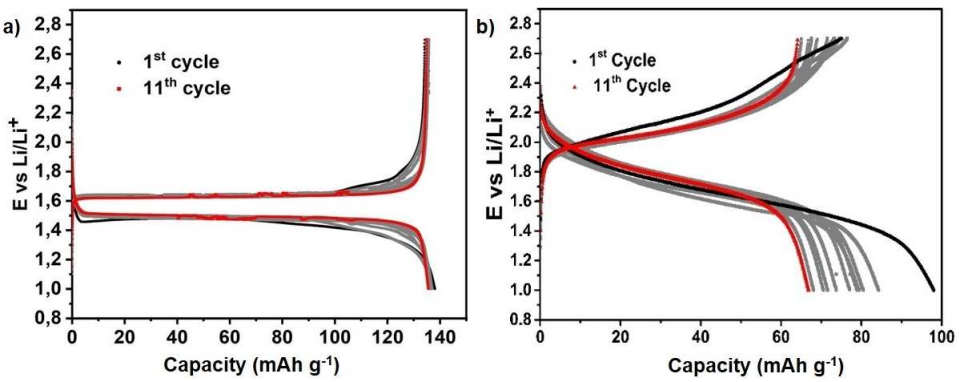

Figure 12. Comparison of electrochemical cycling of pristine (a) and recycled (b) LTO against metallic lithium.

techniques and additives will obviously have an impact on the recycling process. However, one can in principle imagine strategies to overcome such barriers, ranging from crushing of the solid electrolyte via sonification (own unpublished results) to separating of binders such as PVDF via pre-treatment in organic solvents.

From the experiences made on the recovery of materials from ASSBLIBs, we would also conclude that separation processes will have to be well-adopted to a specific combination of materials: such as a combination of LLZTO with $LiFePO_4$ might have to result in a change of strategy or in best case in a use of modified temperatures, concentrations, etc. However, one can see also a strong chance in this – the development of a battery technology which has not entered the market could also be guided by its potential to be recovered efficiently, and this would be a substantial change to the performance guided industrial exploitation of this technology which we face presently.

Acknowledgements

This work has been funded by German federal state of Hessen (Hessen Agentur, HA-Project Number 848/20-08). B.A. acknowledges the financial support by the BMBF (Bundesministerium für Bildung und Forschung) within the FestBatt (Cluster of Competence for Solid-state Batteries) project FB2-Char 03XP0433D. Open Access funding enabled and organized by Projekt DEAL.

Conflict of Interests

The authors declare no conflict of interest.

Data Availability Statement

The data that support the findings of this study are available from the corresponding author upon reasonable request.

Keywords: lithium-ion batteries · solid-state batteries · recycling · garnet · circular economy

[1] J. Duan, X. Tang, H. Dai, Y. Yang, W. Wu, X. Wei, Y. Huang, *Electrochem. Energy Rev.* **2019**, *3*, 1–42.
[2] M. Ghiji, V. Novozhilov, K. Moinuddin, P. Joseph, I. Burch, B. Suendermann, G. Gamble, *Energies* **2020**, *13*.
[3] a) Z. Zhang, Y. Shao, B. Lotsch, Y.-S. Hu, H. Li, J. Janek, L. F. Nazar, C.-W. Nan, J. Maier, M. Armand, L. Chen, *Energy Environ. Sci.* **2018**, *11*, 1945–1976; b) J. Janek, W. G. Zeier, *Nat. Energy* **2016**, *1*, 16141.
[4] B. V. Lotsch, J. Maier, *J. Electroceram.* **2017**, *38*, 128–141.
[5] V. Vanita, A. I. Waidha, S. Yadav, J. J. Schneider, O. Clemens, *Int. J. Appl. Ceram. Technol.* **2022**, *20*, 236–250.
[6] Y. W. Chen-Yang, H. C. Chen, F. J. Lin, C. C. Chen, *Solid State Ionics* **2002**, *150*, 327–335.
[7] Y. Li, F. Wang, B. Huang, C. Huang, D. Pei, Z. Liu, S. Yuan, S. Hou, G. Cao, H. Jin, *Electrochim. Acta* **2022**, *424*, 140624.
[8] S. Siccardi, J. Amici, S. Colombi, J. T. Carvalho, D. Versaci, E. Quartarone, L. Pereira, F. Bella, C. Francia, S. Bodoardo, *Electrochim. Acta* **2022**, *433*, 141265.
[9] a) N. N. M. Radzir, S. A. Hanifah, A. Ahmad, N. H. Hassan, F. Bella, *J. Solid State Electrochem.* **2015**, *19*, 3079–3085; b) F. Elizalde, J. Amici, S. Trano, G. Vozzolo, R. Aguirresarobe, D. Versaci, S. Bodoardo, D. Mecerreyes, H. Sardon, F. Bella, *J. Mater. Chem. A* **2022**, *10*, 12588–12596.
[10] F. Zheng, M. Kotobuki, S. Song, M. O. Lai, L. Lu, *J. Power Sources* **2018**, *389*, 198–213.
[11] J. Lau, R. H. DeBlock, D. M. Butts, D. S. Ashby, C. S. Choi, B. S. Dunn, *Adv. Energy Mater.* **2018**, 8, DOI: 10.1002/aenm.201800933.
[12] V. Thangadurai, D. Pinzaru, S. Narayanan, A. K. Baral, *J. Phys. Chem. Lett.* **2015**, *6*, 292–299.
[13] M. Fingerle, C. Loho, T. Ferber, H. Hahn, R. Hausbrand, *J. Power Sources* **2017**, *366*, 72–79.
[14] a) A. Rajamani, T. Panneerselvam, R. Murugan, A. P. Ramaswamy, *Energy* **2023**, *263*, 126058; b) M. Falco, L. Castro, J. R. Nair, F. Bella, F. Bardé, G. Meligrana, C. Gerbaldi, *ACS Appl. Energ. Mater.* **2019**, *2*, 1600–1607.
[15] A. I. Waidha, V. Vanita, O. Clemens, *Ceramics* **2021**, *4*, 421–436.
[16] A. I. Waidha, T. Ferber, M. Donzelli, N. Hosseinpourkahvaz, V. Vanita, K. Dirnberger, S. Ludwigs, R. Hausbrand, W. Jaegermann, O. Clemens, *ACS Appl. Mater. Interfaces* **2021**, *13*, 31111–31128.
[17] T. Hailu Mengesha, S. Lemma Beshahwured, Y.-S. Wu, S.-H. Wu, R. Jose, C.-C. Yang, *Chem. Eng. J.* **2023**, *452*, 139340.
[18] F. Wu, J. Maier, Y. Yu, *Chem. Soc. Rev.* **2020**, *49*, 1569–1614.
[19] Z. J. Baum, R. E. Bird, X. Yu, J. Ma, *ACS Energy Lett.* **2022**, *7*, 712–719.
[20] T. Raj, K. Chandrasekhar, A. N. Kumar, P. Sharma, A. Pandey, M. Jang, B. H. Jeon, S. Varjani, S. H. Kim, *J. Hazard. Mater.* **2022**, *429*, 128312.
[21] a) K. K. Jena, A. AlFantazi, A. T. Mayyas, *Energy Fuels* **2021**, *35*, 18257–18284; b) J. O. Binder, S. P. Culver, W. G. Zeier, J. Janek, *ChemSusChem* **2021**, *14*, 441–448.
[22] G. A. Blengini, C. EL Latunussa, U. Eynard, C. Torres de Matos, D. Wittmer, K. Georgitzikis, C. Pavel, S. Carrara, L. Mancini, M. Unguru, D. Blagoeva, F. Mathieux, D. Pennington, *Publications Office of the European Union*, **2020**.
[23] L. Schwich, M. Küpers, M. Finsterbusch, A. Schreiber, D. Fattakhova-Rohlfing, O. Guillon, B. Friedrich, *Metals* **2020**, 10, https://doi.org/10.3390/met10111523.
[24] M. Ali Nowroozi, A. I. Waidha, M. Jacob, P. A. van Aken, F. Predel, W. Ensinger, O. Clemens, *ChemistryOpen* **2022**, *11*, e202100274.
[25] S. L. Liu, X. J. Zhao, R. M. Ren, *Adv. Mater. Res.* **2011**, *391–392*, 369–372.
[26] L. Zheng, J. C. Bennett, M. N. Obrovac, *J. Electrochem. Soc.* **2020**, *167*, 130536.
[27] a) A. S. Bastug, S. Gokturk, T. Sismanoglu, *Rev. Inorg. Chem.* **2007**, *27*, 53–65; b) J. Li, Z. Liu, W. Ma, H. Dong, K. Zhang, R. Wang, *J. Power Sources* **2019**, *412*, 189–196.
[28] a) S. C. Yin, Y. H. Rho, I. Swainson, L. F. Nazar, *Chem. Mater.* **2006**, *18*, 1901–1910; b) W. K. Pang, V. K. Peterson, N. Sharma, J.-J. Shiu, S.-h. Wu, *Chem. Mater.* **2014**, *26*, 2318–2326; c) K. Kataoka, J. Akimoto, *J. Ceram. Soc. Jpn.* **2019**, *127*, 521–526.
[29] W. Feng, Z. Lai, X. Dong, P. Li, Y. Wang, Y. Xia, *iScience* **2020**, *23*, 101071.
[30] B. Paul, K. Singh, T. Jaroń, A. Roy, A. Chowdhury, *J. Alloys Compd.* **2016**, *686*, 130–136.
[31] N. Hamao, K. Hamamoto, N. Taguchi, S. Tanaka, J. Akimoto, *Solid State Ionics* **2020**, *357*.
[32] L. Truong, M. Howard, O. Clemens, K. S. Knight, P. R. Slater, V. Thangadurai, *J. Mater. Chem. A* **2013**, *1*, 13469–13475.
[33] W. Zhao, L. Zou, H. Jia, J. Zheng, D. Wang, J. Song, C. Hong, R. Liu, W. Xu, Y. Yang, J. Xiao, C. Wang, J.-G. Zhang, *ACS Appl. Energ. Mater.* **2020**, *3*, 3369–3377.
[34] a) M. Yoon, Y. Dong, J. Hwang, J. Sung, H. Cha, K. Ahn, Y. Huang, S. J. Kang, J. Li, J. Cho, *Nat. Energy* **2021**, *6*, 362–371; b) M. C. Biesinger, B. P. Payne, A. P. Grosvenor, L. W. M. Lau, A. R. Gerson, R. S. C. Smart, *Appl. Surf. Sci.* **2011**, *257*, 2717–2730.
[35] N. Andreu, D. Flahaut, R. Dedryvère, M. Minvielle, H. Martinez, D. Gonbeau, *ACS Appl. Mater. Interfaces* **2015**, *7*, 6629–6636.
[36] G. Assat, D. Foix, C. Delacourt, A. Iadecola, R. Dedryvère, J.-M. Tarascon, *Nat. Commun.* **2017**, *8*, 2219.
[37] Y. W. Tsai, B. J. Hwang, G. Ceder, H. S. Sheu, D. G. Liu, J. F. Lee, *Chem. Mater.* **2005**, *17*, 3191–3199.
[38] B. Lertpanyapornchai, T. Yokoi, C. Ngamcharussrivichai, *Microporous Mesoporous Mater.* **2016**, *226*, 505–509.
[39] R. Djenadic, M. Botros, C. Benel, O. Clemens, S. Indris, A. Choudhary, T. Bergfeldt, H. Hahn, *Solid State Ionics* **2014**, *263*, 49–56.

[40] H. Xu, J. Chen, Y. Li, X. Guo, Y. Shen, D. Wang, Y. Zhang, Z. Wang, *Sci. Rep.* **2017**, *7*, 2960.
[41] M. Huang, T. Liu, Y. Deng, H. Geng, Y. Shen, Y. Lin, C.-W. Nan, *Solid State Ionics* **2011**, *204–205*, 41–45.
[42] J.-P. Schmiegel, X. Qi, S. Klein, V. Winkler, M. Evertz, R. Nölle, J. Henschel, J. Reiter, L. Terborg, Q. Fan, C. Liang, S. Nowak, M. Winter, T. Placke, *J. Electrochem. Soc.* **2019**, *166*, A2910–A2920.
[43] H. Lu, H. Zhou, A. M. Svensson, A. Fossdal, E. Sheridan, S. Lu, F. Vullum-Bruer, *Solid State Ionics* **2013**, *249–250*, 105–111.
[44] a) K. Ozawa, *Lithium Ion Rechargeable Batteries*, Wiley-VCH, Weinheim, **2009**; b) Y. M. Todorov, K. Numata, *Electrochim. Acta* **2004**, *50*, 495–499.

Manuscript received: December 21, 2022
Revised manuscript received: April 2, 2023
Accepted manuscript online: April 8, 2023
Version of record online: May 26, 2023